Multiple reference Fourier transform holography with soft x rays

W. F. Schlotter,[a] R. Rick, and K. Chen
Department of Applied Physics, 316 Via Pueblo Mall, Stanford University, Stanford, California 94305 and Stanford Synchrotron Radiation Laboratory, SLAC, Menlo Park, California 94025

A. Scherz, J. Stöhr, and J. Lüning
Stanford Synchrotron Radiation Laboratory, SLAC, Menlo Park, California 94025

S. Eisebitt, Ch. Günther, and W. Eberhardt
BESSY mbH, Albert-Einstein-Straße 15, 12489 Berlin, Germany

O. Hellwig
San Jose Research Center, Hitachi Global Storage Technologies, 650 Harry Road, San Jose, California 95120 and BESSY mbH, Albert-Einstein-Straße 15, 12489 Berlin, Germany

I. McNulty
Argonne National Laboratory, 9700 S. Cass Avenue, Argonne, Illinois 60439 and BESSY mbH, Albert-Einstein-Straße 15, 12489 Berlin, Germany

(Received 8 July 2006; accepted 6 September 2006; published online 17 October 2006)

The authors demonstrate multiple reference source Fourier transform holography with soft x rays. This technique extends the detection limit of high resolution lensless imaging by introducing spatial multiplexing to coherent x-ray scattering. In this way, image quality is improved without increasing the radiation exposure to the sample. This technique is especially relevant for recording static images of radiation sensitive samples and for studying spatial dynamics with pulsed light sources. Applying their technique in the weak illumination limit they image a nanoscale test object by detecting ~2500 photons. The observed enhancement in the signal-to-noise ratio of the image follows the square root of the number of reference sources. © *2006 American Institute of Physics*. [DOI: 10.1063/1.2364259]

Imaging systems are optimized to reproduce patterns, but when noise accompanies these patterns the image quality degrades. Such degradation due to noise can be usefully quantified as a signal-to-noise ratio (SNR). In x-ray microscopy the SNR can be improved by increasing the exposure time, but this is not always possible. For example, if a specimen is prone to radiation damage, the exposure and thus the SNR are limited by the dose tolerance of the sample. Moreover, in a stroboscopic imaging experiment, the SNR is limited by the number of photons in each single light pulse. The latter case will be encountered in single shot experiments at x-ray free electron lasers, thus requiring that each photon is used effectively.

Lensless Fourier transform holography (FTH) is an imaging technique well suited for high resolution x-ray microscopy as suggested by Stroke and Falconer[1] as well as Winthrop and Worthington.[2] The first experimental realization of lensless FTH was with visible light in 1965.[3] The single shot compatibility of lensless FTH motivated several demonstrations at x-ray wavelengths.[4–6] In FTH the object and reference are located in the same plane and are coherently illuminated. The reference can be generated by a scattering structure, an aperture, or a focusing optic. The interference between the object and reference waves is detected as a hologram in the Fraunhofer region of the object. The spatial Fourier transform of this hologram is the autocorrelation of the two waves and contains an image of the object; this image is the convolution of the object and reference amplitudes. Therefore, the object image can be recovered from the hologram to a spatial resolution comparable to the reference source size. The resolution improves with decreasing reference size but at the expense of object image contrast if there is insufficient reference intensity for good fringe visibility.

Introducing multiple reference sources is a straightforward extension to FTH. In this form of spatial multiplexing, each reference source used to record the hologram will generate a unique image upon reconstruction. At visible wavelengths multiple references have been used for image duplication,[7,8] and for extending the field of view.[9] The effects of multiple reference source interference have also been observed using soft x rays.[10]

In this letter we demonstrate multiple reference source FTH at soft x-ray wavelengths to simultaneously record multiple images of the sample. We show that this method can be used to enhance the image SNR without increasing the energy absorbed by the sample. We apply this enhancement to an image recorded in the weak illumination limit.

We fabricated a nanoscale transmission mask for this proof of principle experiment which builds upon our prior work with soft x-ray FTH.[5,11,12] Since the entire nanostructure defines both the test sample and reference sources we refer to it as the FTH mask. As is shown in Fig. 1, the FTH mask contains a simple block letter F which constitutes the sample. The five holes surrounding the sample define the multiple reference sources. To fabricate the FTH mask, we deposited Au on both sides of a 100 nm thick x-ray transparent Si_3N_4 membrane by magnetron sputtering, then milled the object structure into the Au using a focused ion beam (FIB) system with a 10 pA current of Ga^+ ions at 30 kV. After an additional Au deposition the reference and sample structures were patterned with a FIB. The 1.4 μm thick unpatterned areas of Au are effectively opaque to soft x rays. The backside of the FTH mask is shown in Fig. 1(b) and

[a]Electronic mail: wschlott@stanford.edu

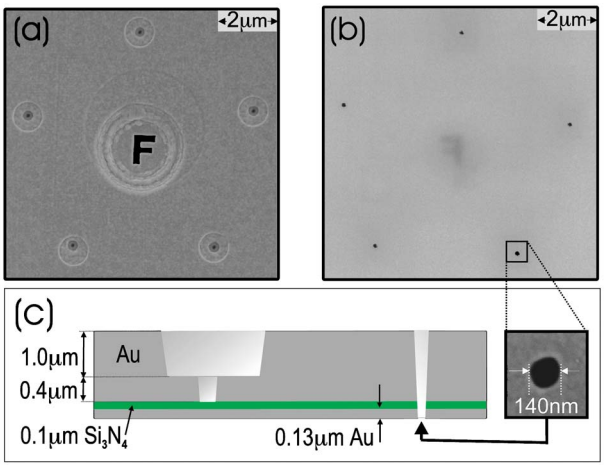

FIG. 1. (Color online) (a) Scanning electron micrograph (SEM) of the FTH mask. The thinned F shape within the recessed object hole is the sample. (b) SEM of the opposite side of the structure in (a) recorded with a 30 kV electron potential reveals a faint image of the sample which is buried below 135 nm of Au. Furthermore, the micrograph confirms that the reference holes penetrate the entire structure. (c) Cross section illustration of the FTH mask including film thicknesses.

contains five uniform reference holes drilled through the entire structure with diameters of 140 ± 6 nm upon penetration. The reference holes are spaced equally on the circumference of a circle with a radius of 4.0 μm. The Si_3N_4 membrane forms the floor of the 250 nm wide trenches which define the F-shaped sample. The intensity transmittance of the F-shaped sample is 12% at a wavelength of $\lambda=1.58$ nm ($E=780$ eV) while each reference has unity transmittance.

The experiments were performed at undulator beamlines at BESSY (UE52-SGM) and SSRL (BL 5-2). In both cases linearly polarized, spatially coherent soft x rays with a wavelength of $\lambda=1.58$ nm illuminated the FTH mask. The small energy bandwidth of the illumination, $\lambda/\Delta\lambda>5000$, defined a longitudinal coherence length of $\lambda^2/(2\Delta\lambda)>4$ μm. The transverse coherence width was $\geqslant 20$ μm. The holograms were recorded by a backside illuminated, thermoelectrically cooled charged coupled device (CCD) camera.[13] At this wavelength the quantum efficiency of the CCD is approximately 80%. The signal created upon detection of a single, $\lambda=1.58$ nm, photon by the CCD is at least an order of magnitude higher than the readout noise. By discriminating the noise below the photon signal, the number of detected photons can be accurately counted. The uncertainty in the number of counted photons results from fluctuations in the CCD signal level for single photon detection events.

The hologram in Fig. 2(a) was recorded with the FTH mask in Fig. 1 with $N_\gamma\sim7\times10^6$ photons. Figure 2(b) shows an enlargement of the fivefold symmetric motif prevailing throughout the hologram. This pattern arises from the arrangement of the reference holes on the vertices of a regular pentagon. The vertical and horizontal bands of higher intensity are indicative of scattering from the rectangular facets on the sample.

Calculating the two dimensional Fourier transform of the hologram generates the spatial autocorrelation of the FTH mask amplitude transmittance. Though the autocorrelation is a complex function we can consider only the magnitude since absorption is the dominant contrast mechanism for this structure. Furthermore, we are interested in the intensity transmittance profile of the sample, as it would be measured

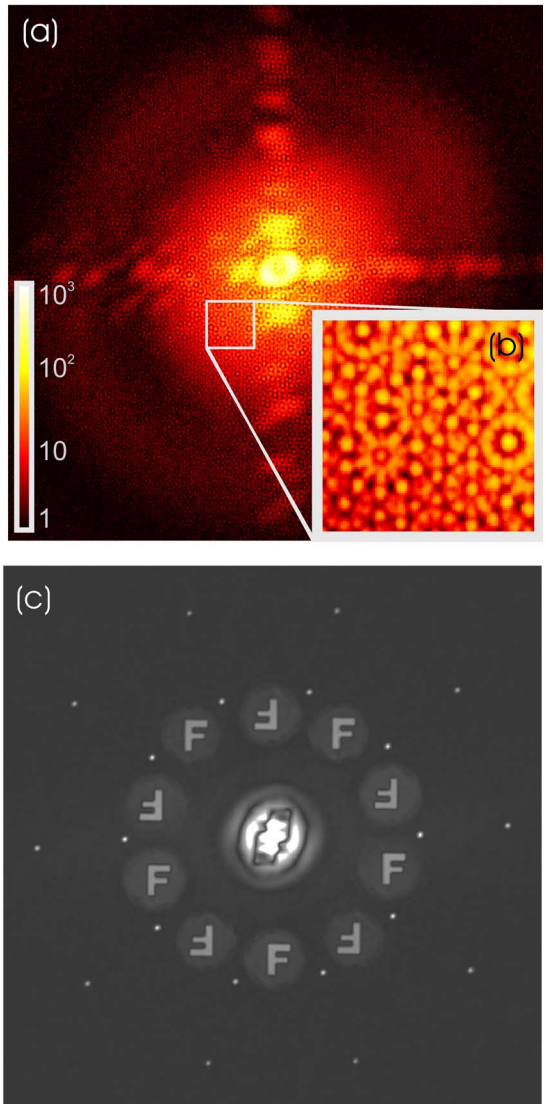

FIG. 2. (Color online) (a) Soft x-ray Fourier transform hologram of the mask in Fig. 1(a). The common logarithm of the intensity is plotted; the scale bar denotes the number of photons detected. The 1200×1200 pixels displayed correspond to a momentum transfer of $q=\pm0.09$ nm^{-1}. (b) Enlargement shows details of the interference pattern characteristics for the five reference sources. (c) Reconstructed holographic images of the sample intensity, i.e., the squared magnitude of the complex autocorrelation.

by transmission x-ray microscopy. This intensity profile is simply calculated, for pointlike references, by taking the squared magnitude of the autocorrelation which is shown in Fig. 2(c). Two redundant images of the sample appear for each reference hole. One image is the cross correlation of the reference with the sample and the other, its complex conjugate, is located radially opposite of the origin. Consequently, the autocorrelation contains five independent images of the sample which, apart from noise, are identical. The center is occupied by the self-correlation of the sample and each reference hole.

The five effectively identical subimages can easily be extracted from the autocorrelation, aligned, and then averaged to generate an enhanced composite image. Since each subimage has exactly the same rotational orientation only Cartesian alignment is necessary, which can be accomplished with a two dimensional cross correlation.

Averaging the subimages improves the image quality, which is particularly beneficial for imaging in the weak illu-

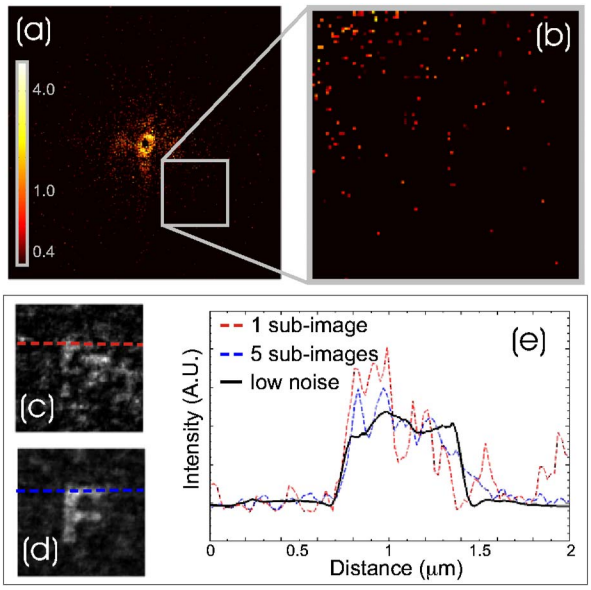

FIG. 3. (Color online) (a) Coherent diffraction pattern resulting from weak illumination of the FTH mask. For clarity only the center part, up to $q = \pm 0.09$ nm^{-1}, is shown; the full pattern used for the reconstruction extends to $q = \pm 0.16$ nm^{-1}. The scale bar corresponds to the number of photons detected in each pixel and is shared with (b) which shows an enlarged section of (a) containing 110 ± 10 detected photons. (c) The sample is very faint in this single subimage where SNR ~ 3. (d) The sample is clearly recognizable in this composite image where SNR ~ 9. (e) Comparison of linecuts through (c) and (d) and a low-noise image similar to Fig. 2(c).

mination limit where the signal of the hologram is dominated by photon noise. Figure 3(a) shows a hologram of the same sample containing only $N_\gamma = (2.5 \pm 0.3) \times 10^3$ detected photons. The characteristics of photon noise are clearly visible in the enlarged region of the hologram shown in Fig. 3(b). Figure 3(c) shows a single subimage of the sample, and Fig. 3(d) depicts the composite image calculated by averaging all five subimages. The linecuts shown in Fig. 3(e), which clearly illustrate the image enhancement, were normalized to have equal background and signal levels for comparison.

The SNR of the images was calculated by taking the mean value $\bar{s}$ of the intensity of pixels comprising the sample and the standard deviation σ_b of pixels in the background surrounding the sample. An equal number of pixels was used for both calculations. Note that in the long exposure, low-noise image the background is flat [shown by the solid line in Fig. 3(e)] as required for determining the SNR which is defined as $\mathrm{SNR} = \bar{s}/\sigma_b$. The improvement in the composite image SNR achieved by averaging N subimages is expected to be $\mathrm{SNR}_N = \sqrt{N}(\mathrm{SNR}_1)$. By comparing the signal-to-noise ratio of a single subimage ($\mathrm{SNR}_1 \sim 3$) with that for composite images using two and more subimages ($\mathrm{SNR}_5 \sim 9$) we see that our data follow this trend.

Remarkably, all of the sample features are resolved in the composite image in Fig. 3(d) which results from only $\sim$2500 detected photons. From the Rose model, which relates the SNR with contrast, resolution, and detected photons,[14,15] the composite image is near the lower limit for discerning the sample at a resolution comparable to the size of the reference sources.

While the performance improvement provided by multiple references is clear, a few details and limitations deserve discussion. (1) The reference holes should be arranged to avoid overlap between the sample images in the autocorrelation. This is achieved when the object can be translated around the entire mask such that it does not overlap with more than one reference at a time.[9] (2) Although using additional reference sources does not increase the exposure to the sample it does augment the detected energy. Consequently, if efficiency is defined by the detected energy, as opposed to the energy absorbed by the sample, the number of reference sources and their intensity transmission are constrained for a given object as described by Mehta *et al.*[7] Though these specifications set boundaries they do not pose any substantial constraints on improvements in imaging performance.

In conclusion, we have demonstrated a SNR enhancement for a spatially multiplexed Fourier transform hologram recorded in the photon noise limit. Remarkably, this improvement is attained without increasing the radiation dose to the sample. The achievable SNR enhancement follows the square root of the number of reference sources. Our results are especially relevant in light of single shot imaging experiments planned for x-ray lasers. Experimental frontiers at these sources will be defined by the photon frugality of the techniques that are applied.

The authors would like to thank H. Zabel for making the ALICE scattering chamber at BESSY available. Portions of this research were carried out at the Stanford Synchrotron Radiation Laboratory, a national user facility operated by Stanford University on behalf of the U.S. Department of Energy, Office of Basic Energy Sciences. One of the authors (I.M.) is supported by the U.S. Department of Energy, OS/BES Contract No. W-31-109-ENG-38, and EU Marie Curie Fellowship MTKD-CT-2004-003178.

[1] G. W. Stroke and D. Falconer, Phys. Lett. **13**, 306 (1964).
[2] J. T. Winthrop and C. R. Worthington, Phys. Lett. **15**, 124 (1965).
[3] G. W. Stroke, Appl. Phys. Lett. **6**, 201 (1965).
[4] I. McNulty, J. Kirz, C. Jacobsen, E. H. Anderson, M. R. Howells, and D. P. Kern, Science **256**, 1009 (1992).
[5] S. Eisebitt, J. Lüning, W. F. Schlotter, M. Lörgen, O. Hellwig, W. Eberhardt, and J. Stöhr, Nature (London) **432**, 885 (2004).
[6] H. He, U. Weierstall, J. C. H. Spence, M. Howells, H. A. Padmore, S. Marchesini, and H. N. Chapman, Appl. Phys. Lett. **85**, 2454 (2004).
[7] P. C. Mehta, C. Bhan, and R. Hradaynath, J. Opt. (Paris) **10**, 133 (1979).
[8] A. Kalestynki, Appl. Opt. **12**, 1946 (1973).
[9] J. W. Goodman and J. D. Gaskill, Proc. IEEE **57**, 823 (1969).
[10] H. He, S. Marchesini, M. Howells, U. Weierstall, G. Hembree, and J. C. H. Spence, Acta Crystallogr., Sect. A: Found. Crystallogr. **A59**, 143 (2003).
[11] O. Hellwig, S. Eisebitt, W. Eberhardt, J. Lüning, W. F. Schlotter, and J. Stöhr, J. Appl. Phys. **99**, O8H307 (2006).
[12] S. Eisebitt, M. Lörgen, W. Eberhardt, J. Lüning, S. Andrews, and J. Stöhr, Appl. Phys. Lett. **84**, 3373 (2004).
[13] Princeton Instruments camera models PI-SX and PI-MTE.
[14] A. E. Burgess, J. Opt. Soc. Am. A **16**, 633 (1999).
[15] A. K. Rose, J. Soc. Motion Pict. Eng. **47**, 273 (1946).